SUPERCONDUCTING MULTICELL CAVITY DESIGN FOR THE ENERGY RECOVERY LINAC AT CORNELL*

Valery Shemelin, Matthias Liepe#
Laboratory for Elementary-Particle Physics, Cornell University, Ithaca, NY 14853

Abstract

The first phase of the Cornell Energy Recovery Linac is the high current, low emittance injector. At present the injector is under commissioning. The next phase calls for the development of the multicell cavity for the main linac. The cavities need to have low RF losses to minimize refrigeration and strong HOMs damping to preserve low emittance and prevent beam break-up at high current (100 mA). Here we present the RF design of the cavity meeting these requirements.

INTRODUCTION

The accelerating cavity for the ERL should satisfy two main requirements: to have low losses and strong higher order modes (HOMs) damping. These two issues are contradictory to some extent because optimization for minimal losses and for maximal HOM damping lead to different shapes of the cells. We decided to optimize the inner cells for minimal losses and sacrifice the losses increase up to several percents in the end cells. The end cells are supposed to be tuned so that they provide propagation of the HOMs into the beam pipes and further to the HOM absorber. Two ends of the cavity will be tuned to different HOM modes; this asymmetry makes possible their better coupling. Besides, the ratio of the peak electric field to the accelerating field in the cavity, aperture of the inner cells and the wall slope angle, see Fig. 1, should be chosen because they also influence on all figures of merit. We chose $E_{pk}/E_{acc} = 2$ and $R_a = 35$ mm deferring experience of the TESLA structure [1]. For the wall slope we chose $\alpha = 95^\circ$. Even smaller angle would lead to smaller losses but we decided not to adopt the reentrant cavity [2] ($\alpha < 90^\circ$); this option should be first more thoroughly tested in a multicell version.

Optimization of cells was done with several modified versions of the SLANS code [3].

LOW LOSS INNER CELLS

For the inner cell we chose the shape with minimal ratio of the peak magnetic field to the accelerating field H_{pk}/E_{acc}. As it is shown in [4], this choice guarantees losses very close to minimal. This shape is uniquely determined if the ratio E_{pk}/E_{acc}, the iris aperture R_a, and the wall slope angle are given. The cell is shaped by two elliptic arcs connected with a straight segment. The cell length is the half-wave length for the work frequency of 1300 MHz; dimensions are shown in Fig. 1 and in the Table 1. The equatorial radius $R_{eq} = 101.205$ mm is the same for both inner and end cells. The ratio of the peak magnetic field to accelerating field $H_{pk}/E_{acc} = 4.02$ mT/(MV/m), the parameter, defining losses, $GR/Q = 15919\ \text{Ohm}^2$, with $R/Q = 58.1$ Ohm in circuit definition.

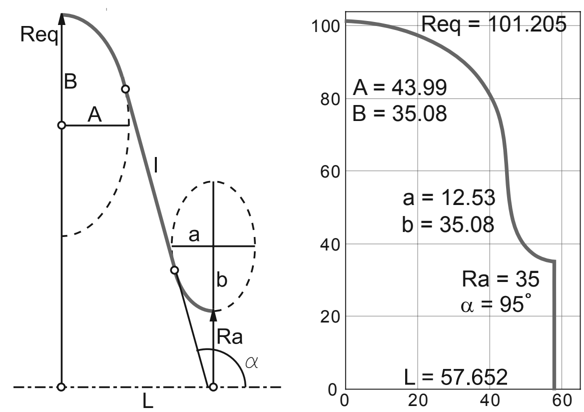

Figure 1. The inner half-cell. Designations and actual shape. Dimensions in mm.

THE END CELLS

The inner half-cells of the end cells have the same shape as the regular inner half-cells. All tunings for HOM propagation are made changing the shape of the end half-cells.

We are considering two versions of the end cells: with and without the iris between the end cell and the beam-pipe. Let's call them the "type *a*" and "type *b*" end cells, see Fig. 2. We will analyze both types of the end cell and take the final decision later when all pros and contras will be clear. Type *a* end cells have narrower beam pipe and thus the cavity can be shorter with the same losses of the fundamental *Q*. Type *b* end cells have a pipe with a lower cut-off frequency and thus better propagation of HOMs with lowest frequencies.

The lowest HOM bands have their frequencies about 1740, 1884, and 2510 MHz, these correspond to the cut-off radii of 50.5, 46.6 mm and 35 mm respectively for the TE_{11} waves in the beam-pipe. Let's choose the pipes with radii 4...5 mm higher than the cut-off radii. So, to propagate the lowest 2 HOM bands, we chose the beam-pipe with radius of $R_{bp} = 55$ mm, and it will be of the type *b*. The iris on the broader beam pipe side helps to improve the shunt impedance of the fundamental mode.

* Work is supported by the NSF grant PHY 0131508 and NSF/NIH-NIGMS grant No DMR-0225180.
# mul2@cornell.edu

For the other end we can choose $R_{bp} = 39$ mm and make it of the type *a*.

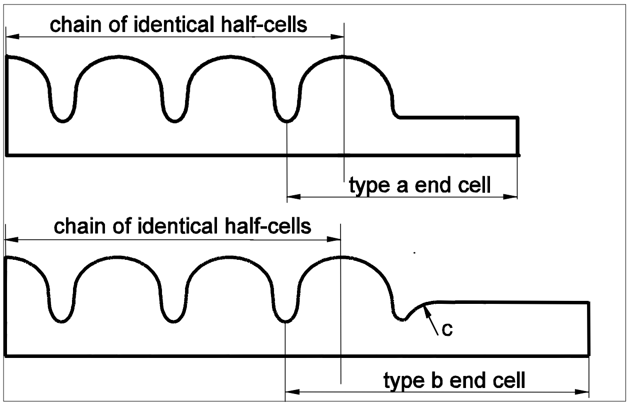

Figure 2. Type *a* and type *b* half-cavities.

Alternatively, both ends can be made of the type *b*. This cavity should have easier tuning for the HOMs propagation but its length will be bigger. For the fundamental TM_{01} mode, the length of 100 dB attenuation between the cavity and the HOM load (needed to keep Q of the SC cavity on the level of 10^{10}) is 336 mm for $R_{bp} = 55$ mm and 208 mm for $R_{bp} = 39$ mm.

Radius *c* of the transition between the end cell iris and the beam-pipe should be big enough, about $c = 2 \cdot (R_{bp} - R_{ae})$, here R_{ae} is the aperture of the end iris. This is necessary to exclude a possibility of multipacting in the minimum of RF electric field which can appear otherwise in this transition [5].

Initial parameters of the end cells are shown in the Table 1. These cells are optimized for minimal losses but further tuning for better propagation of HOMs will change their geometry and figures of merit. We decided to let the end cells to be maximum 7 % worse in the value of GR/Q than their initial versions, i.e. not to worsen the whole 7-cell cavity more than by 2 %.

Besides $E_{pk}/E_{acc} \le 2$ and $\alpha \ge 95^\circ$, two additional restrictions were used for the end cells: curvature radii of the iris $R_c \ge 6$ mm, to exclude manufacturing problems, and the sum of curvature radii on two sides of the end iris $R_{ci} + R_{ce} \le 15$ mm. The last limitation (its exact value can be optional) is necessary because otherwise, in the process of optimization, this iris becomes indefinitely broad, that actually means a narrower pipe with worse propagation of HOMs.

The outer rounding of the type-b end cell iris was taken circular with radius of 6 mm, so for the inner side of this iris $6\text{mm} < R_{ci} \le 9\text{mm}$.

SUPPRESSION OF HOMs

The maximal current in the ERL is limited by beam break-up and is defined by the parameter $p = (R/Q)\cdot(Q/f)$, for single cavity BBU in ERL $I_{max} \propto 1/p$ [6]. For the ERL current of 100 mA this value should be $p \le 1.4 \cdot 10^5$ Ohm/cm^2/GHz for dipoles and $\le 4 \cdot 10^6$ Ohm/cm^4/GHz for quadrupole modes. Taking into account inevitable deformations and errors of manufacturing, these values in the design should be decreased as much as possible [7]. Possible increase of current or/and usage of more than one turn in the ERL also require this decrease. Most dangerous are the dipole modes, so we will discuss here only them.

For the optimization of the shape it is desirable to use an idealized matched load at the ends of the beam pipes in the simulation. We modeled a traveling wave in the pipes and compared the value of the external quality Q_{ext} in this case with a case of solid cylindrical loads at the ends of pipes. The loads were taken as a material with $\varepsilon = \mu = 1 - i$. In the case of a free space such a material gives zero reflection, it appears that in our case, in spite of dispersion in the waveguide, the Q_{ext} does not increase more than 40-50 %. Further transition from a butt load to a hollow cylinder flush with the inner surface of the pipe gives another factor of ≈ 1.4. So, this simulation should not underestimate the actual maximal *p* by more than a factor of 2. Optimization of the load with different ε and μ can be done separately when the best cavity geometry will be found.

The first approach with the initial geometry of end cells gave the map of dipoles shown in Fig. 3 (boxes). For optimization, derivatives of the parameter *p* with respect to each of 8 half-axes (*A, B, a,* and *b* for two ends) were used and maximum *p* was minimized using these derivatives under observance of abovementioned limitations. The result is also presented in Fig. 3 (dots).

In Fig. 4, the associated values of the quality factors are presented.

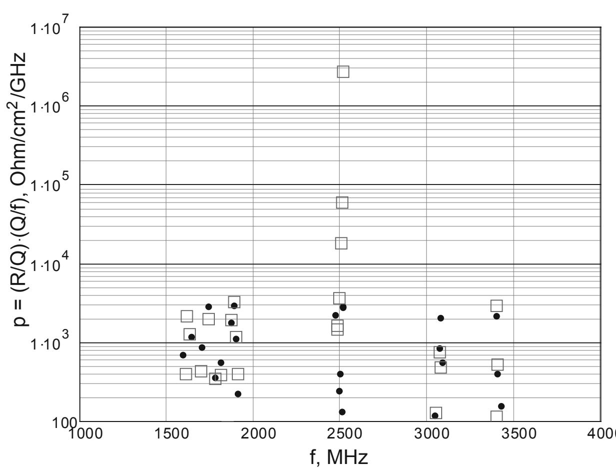

Figure 3. Map of parameter *p* for dipole modes for the initial (boxes) and final (dots) shapes of the end cells.

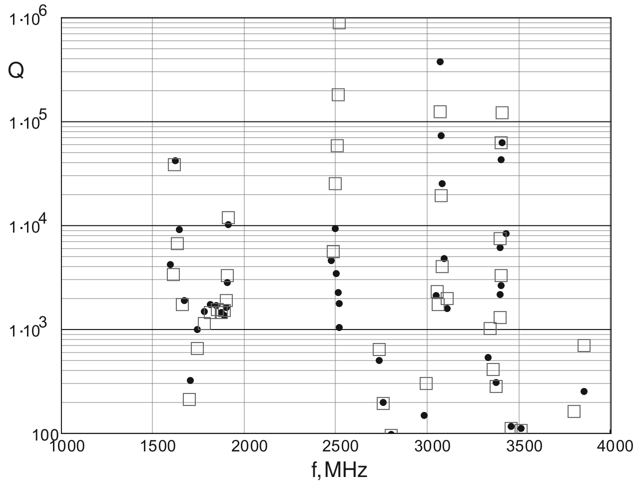

Figure 4. Map of the quality factor Q of the dipole modes for the initial (boxes) and final (dots) shapes of the end cells.

Parameters of the end cells corresponding to these initial and final shapes are presented in the Table 1. Values of GR/Q are given for the whole cell while the end cell consists of the inner half-cell and the end half-cell of type *a* or *b*. As can be seen from the Table, rather small sacrifice of the end cell GR/Q, 4.0 % for the end *a* and 0.9 % for the end *b* was needed to decrease maximal *p* by 3 orders of magnitude. The decrease of the GR/Q of the whole cavity is only 0.7 %.

Higher-Order-Modes with high quality factors not only have the potential to result in high $(R/Q)\cdot(Q/f)$ values in ideally shaped cavities, but also have a significantly increased susceptibility to small deformations and shape errors as a result of cavity manufacturing and surface preparation [7]. Even if tight fabrication tolerances of about 1/8 mm are achieved, remaining shape errors can further increase the quality factors of weakly damped HOMs by several orders of magnitude in individual cavities, compared to an ideal cavity without fabrication errors [7]. Therefore, the presence of real cavities vs. ideal cavities in any real ERL linac could reduce the BBU current threshold significantly, well below the value expected from ideal cavities. Robustness of the HOM damping with respect to small cavity shape errors is thus essential, which results in the requirement that high quality factor HOMs must be avoided, even if their $(R/Q)\cdot(Q/f)$ values in an ideal cavity are not among the highest, and therefore, in an ideal cavity, would not determine the BBU current. In the cavity designs presented here, no high quality factor HOMs above 10^6 are present for frequencies below 4 GHz, see Fig. 4. It is noteworthy, that the improved end cell design not only reduces the maximum *p* for dipole modes below 4 GHz, but also reduces the maximum quality factor Q, thereby improving robustness against fabrication errors.

Table 1. Parameters of the ERL cells.

Parameter \ Cells	Inner cell	Initial		Final	
		End *a*	End *b*	End *a*	End *b*
A, mm	43.99	50.3	51.6	40.6	52.7
B, mm	35.06	44.8	47.4	29.5	44.3
a, mm	12.53	8.4	10.1	21.2	9.6
b, mm	20.95	11.7	11.4	14.0	11.9
R_a, mm	35	39	37	39	37
L, mm	57.652	59.421	62.417	64.909	65.358
GR/Q, Ohm^2	15917	15704	15496	15070	15358

SUMMARY AND OUTLOOK

We have developed an optimization procedure for the main linac cavities in ERL linacs, which achieves strong damping of higher order modes by optimizing the end cells of the cavity, while preserving a high GR/Q value for the fundamental mode. In a preliminary optimization, all dipole modes below 4 GHz have been reduced to $(R/Q)\cdot(Q/f)$ values below $5\cdot10^3$, which is more than a factor of 20 below what is required for an 100 mA, 5 GeV ERL. We will continue this optimization process, and further improvement can be expected. We plan also to further study the robustness of this cavity design to small shape perturbations.

REFERENCES

[1] B. Aune et al., "Superconducting TESLA cavities," *Phys. Rev. Spec. Topics – Acc. and Beams* **3**, 092001 (2000).

[2] V. Shemelin, H. Padamsee, R. L. Geng. "Optimal cells for TESLA accelerating structure," *Nucl. Instr. Meth. Phys. Res. A* **496**, 1-7 (2002).

[3] D. G. Myakishev, V. P. Yakovlev, "The new possibilities of SuperLANS code for evaluation of axisymmetric cavities," PAC1995, May 1-5, 1995, Dallas, Texas, pp. 2348-2350.
D. Myakishev, "TunedCell," Cornell SRF group internal report SRF/D 051007-02, 2005.

[4] Valery Shemelin, "Low loss and high gradient SC cavities with different wall slope angles", *Proc. PAC 2007*, p. 2352-2354, Albuquerque, New Mexico, USA, June 25 – 29, 2007.

[5] Sergey Belomestnykh, Valery Shemelin. "Multipacting-free transitions between cavities and beam-pipes," *Nucl. Instr. Meth. Phys. Res. A* **595**, 293-298 (2008).

[6] G. H. Hoffstaetter and I. V. Bazarov, *"Beam-breakup instability for energy recovery linacs"*, Phys. Rev. ST AB **7**, 054401 (2004).

[7] M. Liepe et al., "*Robustness of the superconducting multicell cavity design for the Cornell Energy Recovery Linac*", these PAC2009 proceedings, (2009).